JAMES COOK UNIVERSITY

SCHOOL OF ENGINEERING

EG4012

THESIS REPORT:
NON-DESTRUCTIVE THICKNESS TESTING USING A UAV COPTER DRONE

Christopher Kellie

Thesis submitted to the School of Engineering in partial fulfilment of the requirements for the degree of

Bachelor of Engineering with Honours

(Electrical Engineering)

October 9th, 2015

Statement of Access

I, the undersigned, author of this work, understand that James Cook University may make this thesis available for use within the University Library and, via the Australian Digital Theses network, for use elsewhere.

I understand that, as an unpublished work, a thesis has significant protection under the Copyright Act and I do not wish to place any further restriction on access to this work.

Signature:___________________

Date:__________________

Declaration of Sources

I declare that this thesis is my own work and has not been submitted in any form for another degree or diploma at any university or other institution of tertiary education. Information derived from the published or unpublished work of others has been acknowledged in the text and a list of references is given.

Signature:____________________

Date:___________________

Acknowledgements

I would like to thank my supervisors Dr David Cole and Dr Kenny Leong for the helpful advice, direction, and pressure that they provided throughout the semesters.

I would also like to thank my engineering peer, Keegan Williams, for his assistance and moral support.

I would also like to thank Brendan Calvert for the use of his wisdom and 3D printing resources. You helped make quick work of what could have been a long process.

I thank my family for their support and encouragement.

Here’s to my housemates Joe, Ramon, Alan, and Kali for their empathy and encouragement.

I would like to thank my lovely girlfriend Christine for being understanding and encouraging during the final weeks of this thesis.

Lastly, I would like to thank any other friends or peers who helped even the smallest bit. Having such a helpful community softens the blow of having to put so many hours into a project. Cheers

Executive Summary

This thesis aims to explore the feasibility of amalgamating concepts from the relatively established Non-Destructive Evaluation (NDE) industry with the emerging UAV industry. Performing thickness testing for uniform corrosion on large, simply shaped industrial vessels using a UAV should increase the spatial versatility of NDE, as well as reducing costs, safety hazards, time, and human involvement overall.

To keep this project within the realm of feasible time and cost, it has to amalgamate the main elements: the UAV, the ultrasonic transducer, and the stability-providing electromagnets. This was done with a custom designed assembly.

The UAV component was tested with software, to simulate the effect of the assembly on the craft, and the assembly side was tested to recreate the effect of the craft on the assembly, as well as its stand-alone efficacy.

The project found the ultrasonic thickness module to be highly sensitive to external factors. The project also found adhesion feasible with electromagnets, that adhesion correlates with instrument weight, vibrations, and surface thickness.

Contents

Word Count: 6393

List of Figures

List of Tables

List of Equations

List Of Abbreviations

NDE – Non-Destructive Evaluation

NDT – Non-Destructive Testing

UAV – Unmanned Aerial Vehicle

PLA – Polylactic Acid

ABS – Acrylonitrile butadiene styrene

Sim – Simulator

VTOL – Vertical Takeoff and Landing

UART – Universal Asynchronous Receiver/Transmitter

1. Introduction

Industrial vessels such as stacks have a high economic value set on their continuing integrity and operation. Routine problems, especially corrosion and weld integrity, pose a threat to this continuing integrity. Industries spend a lot of time and money in order to diagnose and prevent these issues from causing compromise of process or disaster, and ultimately to minimise their economic impact. Non Destructive Tests (NDT) such as ultrasonic thickness testing, ultrasonic diffraction flaw testing, radiographic flaw testing, among others, are used to diagnose trends of corrosion and weld integrity.[1] Corrosion flaws can be of a locally uniform type, or may come in many localised (macroscopic and microscopic) forms as well.[2]

Since such industrial structures are large, and often quite tall, methods have been developed to navigate, test, and tabulate data on these structures in an accurate and non-hazardous way. Generally this is accomplished with workers traversing the structures with scaffolding, elevated work platforms, or rope access.[3] This represents considerable limitations to the efficiency of NDT, mostly in terms of cost and time. An available alternative to this method involves using a rover vehicle with magnetic wheels to take these measurements, reducing labour and set up costs. Such a method does make strides; rovers can take a high density of measurements with accurate encoding, as their slow progression along the vessel allows for accurate position data.

Such rovers are generally tethered to a station that provides control, data processing, power, and irrigation where necessary, allowing for continuous operation. This continuous operation can be encoded in one of a few ways, depending on the transducer type, data of interest, and dimensional parameters of the test.[4]

However, testing with these vehicles comes at the cost of time, since the slow progression of the rovers is very time consuming for a comprehensive test. Such devices are also limited to smooth surfaces; obstructions on vessels will interrupt the continuity of the scanning process.

Emerging Unmanned Aerial Vehicle (UAV) technology has created affordable platforms for aerial imaging, especially in the fields of photography and imaging – both professional and amateur. The affordability of these contraptions has also lent itself to the field of amateur UAV development.

Typical consumer Vertical Take Off and Landing (VTOL) copter drones range wildly in price from around \$50 to \$10000, with commercial models going higher. Most range in between

400 and 3000 grams, depending primarily on the number of rotors. Unloaded flight time is usually at least 8 minutes, with varying payload capabilities of up to a kilogram.

The versatile nature of the UAV platform makes it a compelling means of hosting NDT tools. Such a highly manoeuvrable vehicle could conceivably not only increase the rate at which NDT is carried out, but also the possible places. A UAV that could fly up and perform NDT at an altitude of 100m, especially in a short time, augments many possibilities that are not currently possible or feasible.

2. Literature Review

2.1 Non-Destructive Evaluation

2.1.1 Ultrasonics

In the NDT realm, ultrasonic testing (UT) is one of the more prevalent methods of executing test. Its ubiquity can be attributed to its versatile nature. There are many types of ultrasonic testing methods, including acoustic resonance testing, electromagnetic acoustic transducer testing, laser ultrasonic testing, phased array ultrasonic testing, ultrasonic time of flight diffraction testing, Schlieren tests, and thermal or radiation force activity receiver type tests, among others[5]. These typically work at ranges of from 200 KHz up to 10 MHz. At such high frequencies, UT is able to detect flaws at a macroscopic level, provided they are not parallel to the direction of wave propagation. [1]

There are several ways to orient the transducers for normal incidence UT, though they will be some variation of one of two setups. The first is Direct or Through method, which involves two transducers (one acting as a transmitter and one as a receiver) on opposite sides of the media and the second is Pulse-Echo method, where the same transducer transmits a pulse into a medium and receives the corresponding echo shortly after. In the field, the Direct method is problematic to implement, so a Pulse-Echo setup is the only viable option.

UT is generally used for testing for macroscopic flaws such as pitting corrosion or procurement defects, but it is not uncommon for it to be used for testing the dimensional thickness of a material. Certain imaging methods that are intended for finding transverse flaws also include a fairly clear indication of medium boundaries.

Commonly established imaging methods for normal incidence UT include A-Scans, B-Scans, and C-Scans. A-Scans represent the reflection strength vs time at a single point (0-Dimension), indicating both discontinuities and boundaries of a single point scan. B-Scans represent a series of A-Scans encoded against 1-Dimensional movement. Typically, the Cartesian plane is reserved for 1-Dimensional translation (x), time (y), and the signal strength is plotted as a colour gradient. C-scans represent a planar (2-D) scan, where some amplitude metric is plotted as a colour gradient. Supplementary A-Scan data is available for each evaluation point. [6, 7]

These imaging methods are also suited to image data recovered from an array of transducers. Phased arrays consist of a series of ultrasonic transducers that can be activated in series or combination to recreate dimensional translation or use the interference to create an anisotropic vibration pattern.

An ultrasonic transducer consists of a housing, an active piezoelectric layer, a wear plate and a backing material layer (generally much thicker than the active piezoelectric layer. The properties of these layers are very important to the function of the transducer. All of these layers have a characteristic impedance Z that relates wave velocity and pressure:

$$Z = \frac{P}{v} = \rho . c \qquad (2.1.1a)$$

Where P is particle pressure
v is particle velocity
ρ is the medium density
c is the speed of sound in the medium

At the boundary between two media, both the particle pressure and particle pressure are continuous, else they would cease to be in contact. Due to this property, not all of the energy in a sonic wave will be transmitted between two media with different characteristic impedances. Some fraction of the incident energy will be reflected per the equation

$$R = \frac{Z_2 - Z_1}{Z_2 + Z_1} \qquad (2.1.1b)$$

It is therefore important to match the media the wave is to travel through as best as possible. As the wave travels through the wear plate, coupling medium and testing medium and returns back, a large amount of the incident energy is capable of being dissipated. The wear plate will generally match the impedance of the active piezoelectric element. How well matched/damped to the active piezoelectric layer the backing layer is is an exchange of instrument sensitivity and penetrative power; a poorly matched backing layer will reflect the energy towards the testing medium, but a well matched backing element will increase the bandwidth and overall sensitivity of the transducer.

The coupling medium is an important aspect of the testing setup as well. In many circumstances, air would be a very convenient coupling medium, though its characteristic impedance is quite different to that of steel or piezoelectric, thus the transmission coefficient is very low between media. Irrigated water is a ubiquitous medium, though this proves a problem for a mobile platform. Other dry coupling media are available, such as Silverwing NDT's rubber wheel.[8]

2.1.2 Rovers

Current Rover/crawler solutions are able to adhere to a steel vessel with magnetic wheels, and perform A, B, or C ultrasonic scans, depending on their encoder capabilities. Some of these appliances have a dry or wet coupling method. Wet coupling methods, such as an irrigated water method, will require a tether, sometimes referred to as an umbilical cord.[8]

2.1.3 Corrosion

Corrosion can happen in many ways. In the basic sense, an object can exhibit three kinds of behaviour with respect to corrosion:

- Immune behaviour, where the material is generally unaffected by neighbouring electrolytes.
- Passive behaviour, where initial corrosion occurs, but results in an insoluble protective film that greatly slows the rate of reaction.
- Active behaviour: a reaction occurs and produces a soluble, non-protective layer. Characterised by high material weight loss.

Corrosion is best categorised hierarchically, shown:

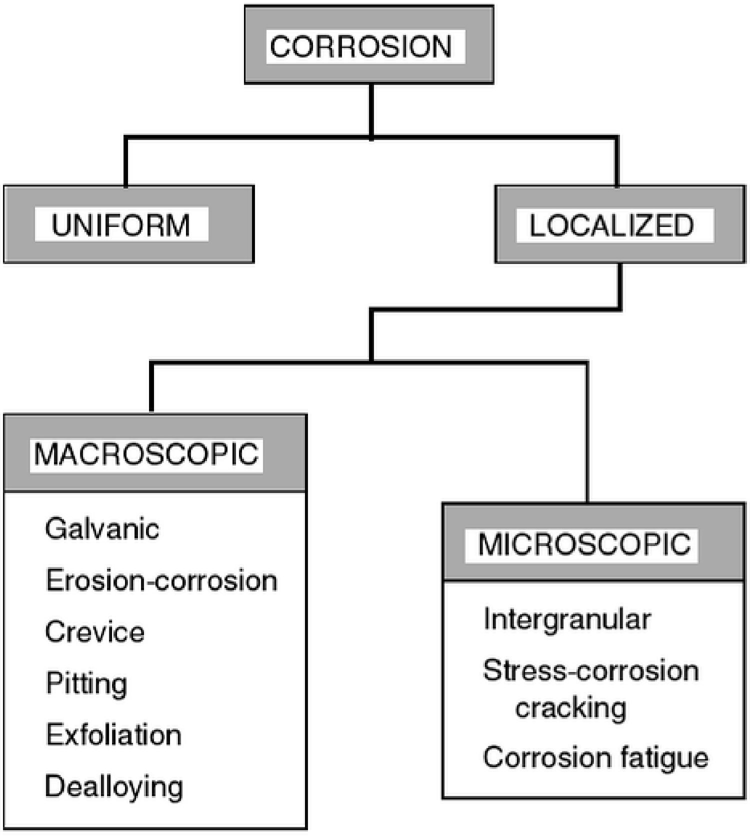

Figure 2.1.3a Corrosion Hierarchy[2]

Thickness testing will focus on diagnosing uniform corrosion. Though it is possible that if the quality of information is high enough, the craft may be able to test for certain macroscopic defects as well, such as pitting, or regions of dealloying.

2.2 UAV TECHNOLOGY

2.2.1 System overview

Multirotor copter are afforded their popularity by a few factors, including their versatility, low cost, lack of swashplate mechanism, relative simplicity to design, among other things. [9]

They consist of a frame, motors, rotors, speed controllers, IMU, control electronics or flight computer, CPU, and other peripherals such as a camera or radio link.

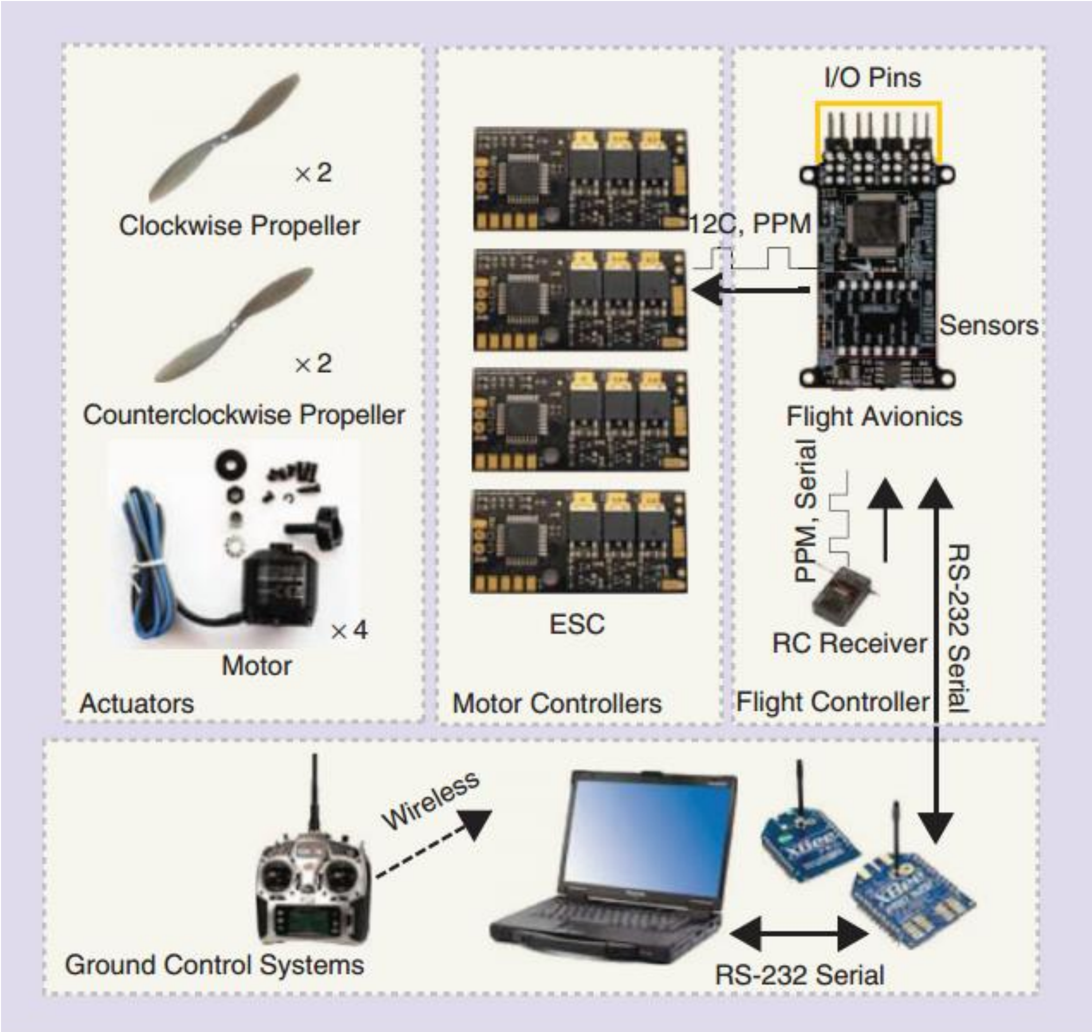

Figure 2.2.1a: Quadcopter Drone Components

There is a considerable DIY scene – 8 popular open source platforms exist that use popular processors.[9]

For a quadcopter in a steady condition, all of the rotors are at the same speed. To climb or descend, the rotors all speed up or slow down. To translate, the craft changes its pitch and roll such the vertical component is thrust is equal and opposite to gravity, and there is some horizontal component of acceleration. Pitch and roll are changed by slowing the motors on one side compared to the other side, in order to create an uneven moment on the craft. Of these motors two will be spinning clockwise, and two will be spinning counter clockwise. Motors diagonally opposite will be spinning the same direction. Yaw is changed by slowing one of these diagonal pairs in relation to the other opposite pair, thus causing a net moment about the vertical axis. In copter with more than 4 rotors, this becomes less straightforward, but the concept of altering the moments stays the same.[10]

In order to limit transient noise and steady state drift, the flight computers must implement a Partial-Integrator-Differentiator (PID) control system. Copter platforms do this with varying levels of automaticity.

2.2.2 Navigation

2.2.2.1 GNSS

In order to orient themselves to the earth, objects can utilise what is known as a Global Navigation satellite (GNSS) system. These systems use simplex (unidirectional) UHF communication. They function by sending a time signal from several satellites with predictable orbits and using a receiver within atmospheric line of sight to use this information to deduce a latitude, longitude, altitude, and a synchronised clock value.

The most prevalent GNSS is GPS (Owned by the US military), though other systems exist. Russia owns and operate GLONASS, and China has the BeiDou system, with other systems in development by the EU and other countries. These all have varying degrees of accuracy, from within 8 metres (free access) down to 10cm (with licensed use). Australia has widespread use of GPS, which will be used in the project’s aircraft.

GPS technology in its current state does not provide suitable accuracy for the use of encoding the measurements taken. It does serve as a useful means of vague orientation against a vessel, though with CEP (50% of measurements within a radius of) values of 2.5m or greater on many units, this technology is limited to this application. Proposed GNSS systems may change this dynamic, however. It is for this reason that other complementary relative position and inertial measurement units are necessary in order to increase the accuracy to a meaningful value.

2.2.2.2 IMU

The IMU is essential to the stable function of the aircraft. It provides attitude (pitch, roll, and yaw) information of the craft at a high rate in order for system to remain in a state of transient stability, and possibly to minimise its steady error, if the system has implemented the control systems for it. It will also be necessary for the purpose of orienting the craft against the vessel it is testing.[9]

Its function consists of MicroElectroMechanical Systems (MEMS) that make up an accelerometer and gyroscope, as well as a magnetometer unit. Collectively, these units provide a 3 axis reading of acceleration, a 3 axis reading of magnetic field, and a 3 axis reading of differential position. From the measurements of the compass and accelerometer, a bearing is obtained. The gyroscope is useful in the event that the other two sensors have some loss of signal or signal quality.

Each is with their respective drawbacks. Movement and vibration of the craft causes acceleration that may need to be filtered from the accelerometer data. An aircraft will use electrical motors that, without proper shielding, will affect the magnetic field that the magnetometer will detect, potentially causing loss of signal quality, and increasing signal processing requirements. The magnetic field may also be skewed by external factors such as inductive power loads or redirection of the earth's magnetic field through a large structure. A gyroscope is generally immune to these sorts of effects since it only takes internal measurements, though this characteristic (Dead reckoning) comes at the cost of steady state bias. A regular calibration may need to be executed.

2.2.2.3 Altimeter

Often a GPS is even less accurate in the altitude dimension than it is in latitude or longitude. Although bearing information can be supplemented to some degree by an IMU, this capability is not very accurate. It is highly beneficial to have a supplementary altimeter, and for the purposes of this project, necessary. Some stock crafts may come with some form of altimeter installed.

Barometer based altimeters are very common and quite cheap. Hobbyist models can cost about $10 and work up to 1km above ground level with an accuracy of about 30cm, which is not ideal, but is far better than what GPS can offer. Other limitations include fluctuation with temperature and humidity.

Detection and Ranging systems (such as RADAR and LIDAR) can also be used for these purposes, though they require a direct path to the ground and back. At lower ranges (<40m), LIDAR works at a higher accuracy than a barometer (a single digit centimetre accuracy), but this may not suit the heights of the project intends to cover. Sensors of this kind are also quite expensive, possibly costing more than half of the thesis budget. RADAR also has this shortcoming, though due to a lower SNR, has about the same accuracy as a barometer altimeter. RADAR often has large and powerful antennas as well.

2.2.2.4 Ad-Hoc Local Positioning Systems

As well as sensors that measure static characteristics in order to discern bearing or position, there are a variety of ad-hoc sensor network local positioning systems that use characteristics relative to each other to discern bearing or position. Generally these systems are geared towards indoor environments where measuring GPS and other characteristics is troublesome. There are many of these available, though this review will limit the representation to three prominent, but different methods.

The ZigBee RSSI (Received Signal Strength Indicator) Indoor Local Positioning System [11] uses the inbuilt signal strength indicator to scope distance by relating reducing signal strength to distance. A ZigBee mesh will have an extensive range of these measurements relative to each other updating at some frequency, so a signal processing method such as Euclidian distance method, or a neural network algorithm needs to be implemented. The obvious disadvantage of this characteristic is that a powerful processor is needed to process all of the measurements, though this is common to most ad-hoc positioning systems. RSSI methods are also quite susceptible to multipath effects.

The Cricket Indoor Location System [12] uses a combination of RF and ultrasonic waves and uses the Time Difference of Arrival (TDOA) to discern the proximity of a node. However, this method is not particularly versatile, as the ultrasound wave is limited to line of sight applications in acoustically hospitable conditions. At ranges expected in this project, implementation of this system would be inappropriate.

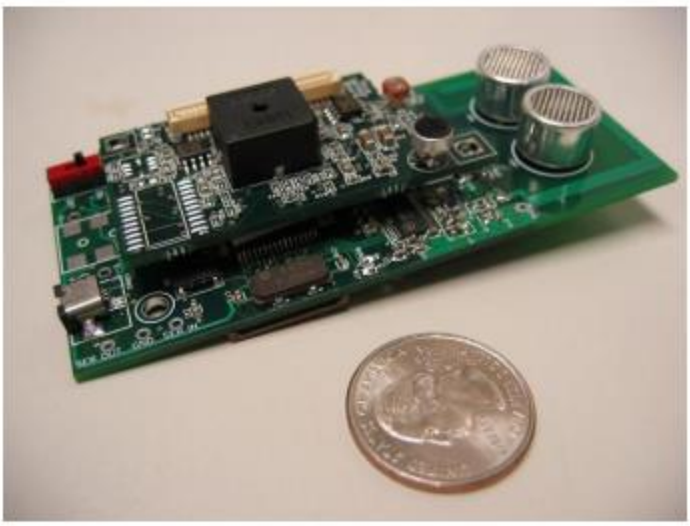

Figure 2.2.2.4a Cricket module

Ad-hoc Angle of Arrival (AoA) methods can also be used to triangulate and trilaterate an object. Put simply, the system uses an array of directional antennas in order to discern the angle to some node. If the AoA of 3 nodes with known positions is known, the location can be found through trigonometry. Disadvantages of this method include the complexity of the antenna arrays, and that the error of the angle measured actually depends on the angle itself, resulting in a nonlinear error. This would prove troublesome in an air to ground situation where the nodes are at similarly shallow angles.

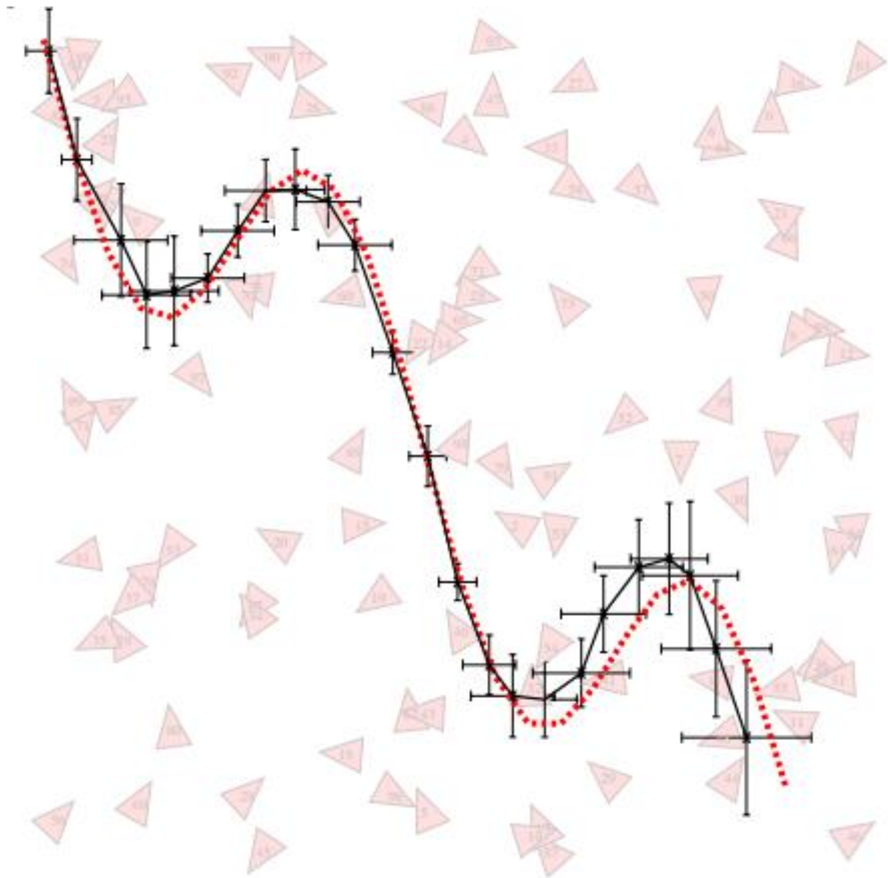

Figure 2.2.2.4b AoA Isotropic Tracking Map

Methods such as these are not particularly useful in a low duty cycle outdoor application, due to distance and power limitations, interference, lack of fastening points, and low economic feasibility.

2.2.2.5 GNSS-Denied Environment SOlutions using sensor odometry

There are some solutions that do not make use of global or local systems in order to determine a location. These systems typically make use of pre-existing sensors on the craft, including the IMU and Detection/ Ranging systems. Some designs incorporate the use of one or more cameras as well.[13] Many of these systems work on a principle called SLAM (Simultaneous Location and Mapping), which has these sensors using feature detection to attempt to mitigate the error in a system with no absolute position information available.

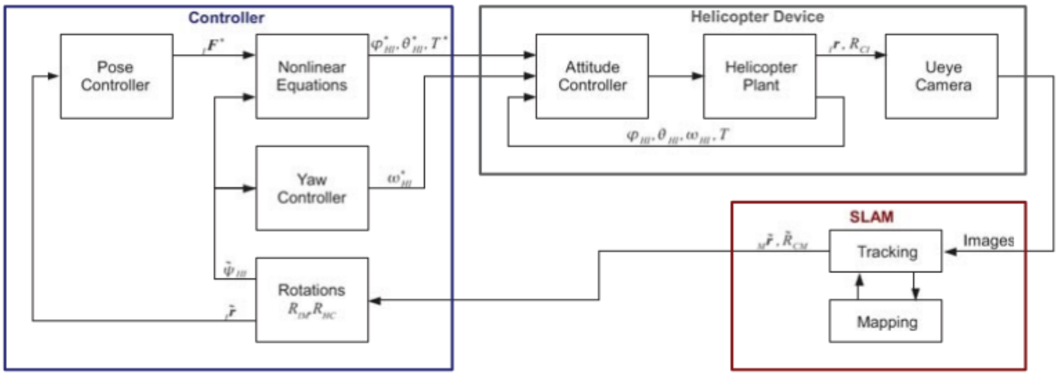

Figure 2.2.2.5a: mono vision slam integration block diagram[13]

The SLAM system has the complex responsibility of fitting the tracking and the mapping information together in order to be effective. MIT's *Stereo vision and laser odometry for autonomous helicopters in GPS-denied indoor environments* outlines how this is done by combining IMU and exteroceptive information and relaying this to a base station with more computational power. The base station calculates a global map, which the copter can compare its control loop states against.[14]

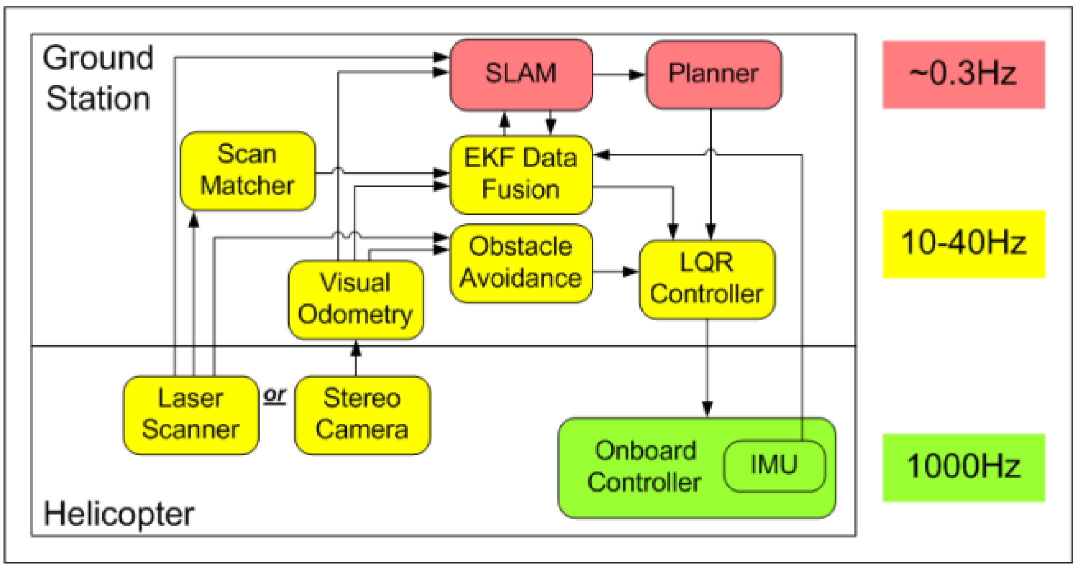

Figure 2.2.2.5b Stereo camera processing flowchart[14]

A design in other literature make use of a ZUPD (Zero Velocity Update), which calibrates the first integral of the IMU (velocity) to zero in conditions where it is known to be zero. A repeatable means of calibrating the velocity error reduces the velocity function to a type 1 system (finite steady state error), reducing the overall drift of the position information over time. The design (a shoe affixed IMU odometry system) proved to have about 2-3% error over 400m of walking.[15]

2.2.3 Collision avoidance and UAV preservation

Though LIDAR and ultrasonic distance sensors are not preferable solutions for altitude ranging, they are very desirable sensor platforms for short distance ranging. They are quite accurate at short ranges as well. These sensors can be used for both collision detection and to supplement telemetry.

Certain UAVs, such as the Parrot AR.Drone 2.0 incorporate the use of a hull or propeller guards in order to preserve the UAV in the result of a collision. If a collision occurs, the propellers will be preserved and the aircraft can be manoeuvred to a safe place if it is damaged.

2.2.4 Legal

The Civil Aviation Safety Authority (CASA) discerns the difference between Remotely Piloted Aircraft (RPA) and a model aircraft as: Any craft of any size used for commercial, government, or research purposes is classed as an RPA whereas model aircraft are flown for sport or recreation.

Flying an RPA for commercial reward requires a UAV controller's certificate and an unmanned operator's certificate for the business.

Without CASA approval and licensing, Aircraft cannot fly more than 400 feet above ground level (in controlled airspace), within 30 metres of buildings or vehicles without permission of the owner, outside of visual meteorological conditions(outside line of sight), within 5.5km of an airfield, or over populous areas such as beaches, heavily populated parks or in use sporting ovals.[16] This provides a limitation to the possibility of the project

2.2.5 Perching

There is some research and design perching technology (especially for a larger craft). The available resources did indicate a few novel concepts.

The first was not necessarily a perching mechanism, but does have merit in the testing that is to occur. UDC's boiler inspection UAV (the MAGNEBOT) has a custom designed frame with four protruding arms with wheels on the end.[17] These wheels slot between grooves in a tube-wall commonly seen in boilers. This provides it with planar stability, leaving the craft with one dimensional degree of freedom – altitude. However, the innovation is currently only used for visual inspection, where the actual camera and electronics are offset from the wall by about 2 feet. A similar design could greatly increase the robustness of the encoding if the craft were able to use wheels to determine a change in position.

The second is a joint project between the University of Maryland's Autonomous Vehicle Laboratory and Stanford's Biomimetrics and Dexterous Manipulation Lab (BDML). The project has created a small quadcopter with a perching mechanism affixed. The mechanism uses a dry adhesive which incorporates biomimicry of gecko feet (using van der Waals forces) and a tendon and ratchet mechanism. Demonstrations show the contraption adhering to two horizontal surfaces: a floor and a ceiling, with the ability to continue to adhere at any angle between the two. [18]

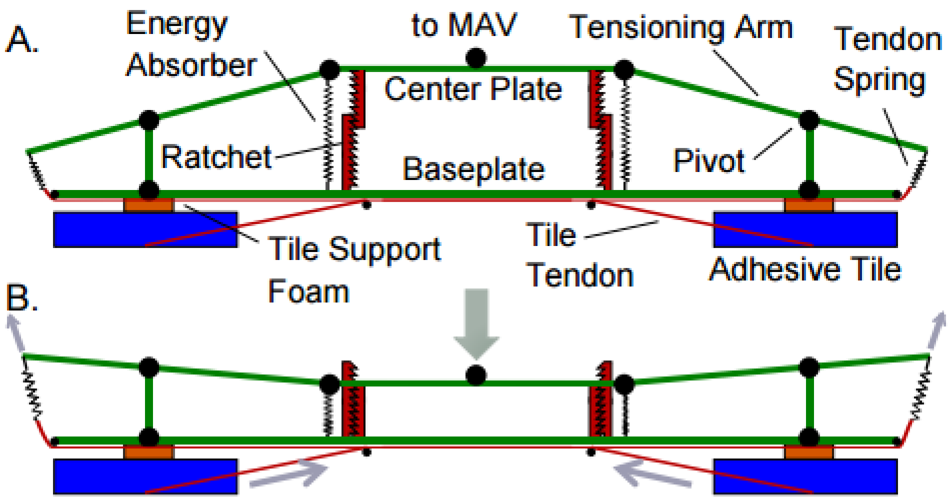

Figure 2.2.5a BDML Adhesive Mechanism

2.2.6 Simulation

Many flight and robotics simulators are available, with varying prices, intended applications, and ease of development. X-planes, FlightGear, and Microsoft Flight Simulator are considered to be some of the better applications for flight simulation and training [19]. X-planes is often praised for its utility for prototyping purposes as a Hardware-In-the-Loop (HIL) simulator, as its use of blade element analysis affords it high physical fidelity[20]. However, availability of relevant flight models is limited, and development comes with considerable learning curves and proprietary software costs. Robotics-focused simulators (such as ROS, Webots, and USARSim) also have a mix of similar abilities and limitations. These simulators are generally limited towards assembly line or ground based mechatronics, and do not aptly facilitate a simple multicopter UAV simulation.

SimMechanics (a toolbox for MathWorks' Simulink) is a popular platform for development and simulation of flight controllers for UAV. It provides a simple control systems approach to designing and implementing simulations of many simple non-ballistic physical applications. It has the inherent advantage of piggybacking upon MATLAB's and Simulink's smorgasbord of control systems analysis tools. Since there is no finite element dynamics engine available, certain kinetic properties need to be manually defined. In the case of a simple Multicopter UAV model, this is a thrust vector for each propeller, related to propeller angular velocity by equation 2.2.6.1 [10, 21]

$$T = \left(\frac{K_v K_\tau \sqrt{2\rho A}}{K_t}\omega\right)^2 = k\omega^2 \tag{2.2.6a}$$

SimMechanics has an abundance of third party UAV models available. Of the many examples, Khanh Dang has provided a meticulous model of the DJI F450 under a BSD copyright license[22]. This model demonstrates a simple flight plan consisting of non-concurrent changes in altitude, yaw, pitch and roll. This forms a suitable base model to alter in order to simulate how the load of a transducer and assembly may affect UAV flight dynamics.

There is literature available that mentions, from fundamentals, how to approximate power usage using quadcopter dynamics and intrinsic part values, shown in equations 2.2.6.3-2.2.6.4 [21]

$$P = IV = \frac{(\tau + K_t I_0)(K_t I_0 R_m + \tau R_m + K_t K_v \omega)}{{K_t}^2} \tag{2.2.6b}$$

$$\approx \frac{(\tau + K_t I_0) K_v \omega}{K_t} \tag{2.2.6c}$$

$$\approx \frac{K_v}{K_t} \tau \omega \tag{2.2.6d}$$

In order to simulate a mass that attaches to the UAV, a shape needs to be defined. In SimMechanics, this can be represented by any shape. The simplest is a sphere, defined by a stereo-lithography file, a mass and, a moment of inertia. Moment of inertia for a sphere of uniform mass is defined by equation 2.2.6.5 [23].

2.3 Regression Analysis

In order to quantify the effect of one or more variables on a certain outcome, a mathematical analysis is necessary, to discern how the variation of predictor variables affects the probability of outcome variables. There are many kinds of regression analysis for many different data types.

Since the hardware simulation has two simulated inputs, it is considered to be a multivariable system. It has two binomial outcomes and one outcome variable that is expected to be ordinary.

Logit or probit models could be used to model the binomial outcomes variable against the multiple predictor values [24]. However, using these methods in a multivariable context is not well established. Thus the use of a linear model to model a discrete situation such as this is suitable, accepting that the partially "mathematically nonsensical" results will require a sensible human interpretation.

Brown [25] mentions that using a multivariable linear least squares regression method aims to get a solution of the form

$$y_i = \sum_k [\beta_k x_{ik}] + \beta_0 + e_i \ , i = 1,2,3 \ldots \quad (2.3a)$$

MATLAB's Statistics and Machine Learning Toolbox has many functions that can perform this analysis easily.

2.4 Conclusion

2.4.1 Perching for larger craft

The literature leaves something to be desired for the purposes of perching with a VTOL multicopter aircraft to a vertical surface. The concept of electropermanent magnets seem most suitable for the application of a perching VTOL multicopter, but are not well developed enough to be deployed in this project. Ordinary electromagnets will need to be used, despite their relatively high energy requirements, and weight.

2.4.2 Copter Drone mounted NDT transducer assembly

The literature has little to no relevant mention of a multicopter assembly that houses NDT transducers. A simple one will need to be created with simple, non-expensive materials and methods such as wood carving or 3D printing (PLA or ABS).

2.4.3 Weight capacity vs time of flight

There is also limited empirical information on how the payload weight affects the time of flight of a VTOL Copter Aircraft. Under ideal conditions, this can be approximated using quadcopter dynamics and intrinsic part values.

2.4.4 Simulation

The most suitable means of simulating and/or developing control systems for a simple NDE tool laden UAV is with the SimMechanics toolbox for Simulink.

2.4.5 Regression

A linear regression model (such as least squares) can be used in spite of a binomial output, though some ‘human interpretation‘ will be required to evaluate these results.

3. Project Intent

3.1 Aim

The ultimate objective of this thesis was to have a working design capable of autonomously taking thickness measurements within a minimal time frame with minimum human supervision. It is immediately obvious that such an objective is multifaceted and not without an expansive scope. It is for this reason that the project scope has been limited and prioritised by merit of:

- Application sequence (the order of actions that the finished product will execute)
- Perceived development opportunity
- Achievability

Thus, the precedence of the explored aspects of this thesis, in descending order, was:

To explore the feasibility of creating dimensional stability against a vertical surface with a VTOL copter drone with either a magnetic perching mechanism.

Another underlying issue of the VTOL copter drone is that the platform excels due to the minimalistic weights of the vehicles. The possibility and practicality of carrying all of the necessary appliances will be need to be investigated, in order to discern how the payload will compromise aspects of the craft such as manoeuvrability and flight time. This was done using a combination of simulation software and control algorithms.

3.2 Scope

There are a variety of sensor types. Alternative NDT methods and transducer types such as Ground Penetrating Radar and Acoustic resonance testing do exist, though unlike prevalent ultrasonic transducer types, these generally have bulky assemblies or unusual physical requirements making them hard to cater for in mobile applications, especially robotics. For this reason, the design was limited to the well-established thickness testing method of a piezoelectric transducer implemented as a pulse-echo A-Scan module.

The project had intended to use a pre-existing copter design, however due to availability and budget issues, the multicopter facet of the project was limited to simulation, and only the assembly was physically simulated.

The craft was limited in operation to testing the outside of the vessels using a pulse-echo testing method. In the hardware simulation section of this project, this was represented as a flat plate of metal (holding the assumption that the vessel has a flat surface, or one with a large enough radius to make it effectively flat). It is possible that the sister project (Internal Inspection UAV) may facilitate NDE of insides of vessels at some point, but it was a concurrent development, so there was little room for integration.

4. Methodology

4.1 Design of Experiments

4.1.1 Transducer Assembly Hardware Simulation

This experiment used:

1. A 3D printed assembly made of PLA(2 pieces)
2. Two steel plates(of thicknesses ~1.5mm and ~10mm) to simulate a wall the assembly would perch/fasten to
3. 2 vibration motors in order to simulate vibrations that a uav might introduce
4. 3 50N lifting electromagnets
5. A Benetech GM-100 5MHz Digital Ultrasonic Thickness Gauge
6. M20 Hex nuts to simulate the weight of the UAV
7. M20x300mm bolt to simulate the weight of the UAV
8. An Arduino Mega2560 to control the electronic components via UART
9. 5 logic level N-channel MOSFETS to switch the electronic components
10. A Standard ATX computer power supply to power the electrical components
11. A computer running PuTTY to interface with the Arduino Mega2560 over UART
12. Wood screws to hold the 3D printed pieces together

The 3D models were designed and rendered in OpenSCAD, and printed by Brendan Calvert. There was some dimensional contraction apparent, due to the nature of 3D printing, so these issues were rectified with hand tools, so that the electrical parts (3, 4, and 5) would fit snugly into the assembly. The 2 3D printed parts were fastened with woodscrews, and the weights were hung off of the assembly at a distance of 45mm from the surface of the steel plate. The electrical parts were attached into a breadboard attached to the Mega2560. This assembly was attached to the steel plates, where it was tested for

- Its ability to adhere to the surface(Binomial outcome)
- Its ability to successfully couple the transducer to the surface(Binomial outcome)
- The recorded thickness(ordinary outcome, as an error)

Against

1. Varied weight applied to the assembly
2. Varied Vibration intensity applied to the assembly

The weight was applied in intervals of 58 grams from 390 grams of 1318 grams and the MOSFETS controlling the vibration motors were alternately incremented by 10% duty cycle at a time, from 0 to 100% of a 12V supply signal.

The thickness and coupling information can be recorded from the GM100 module. The top-left symbol represents a successful coupling, and the thickness is displayed in mm, shown:

Figure 4.1.1a: Ultrasonic Thickness Gauge Display

The overall design setup, shown:

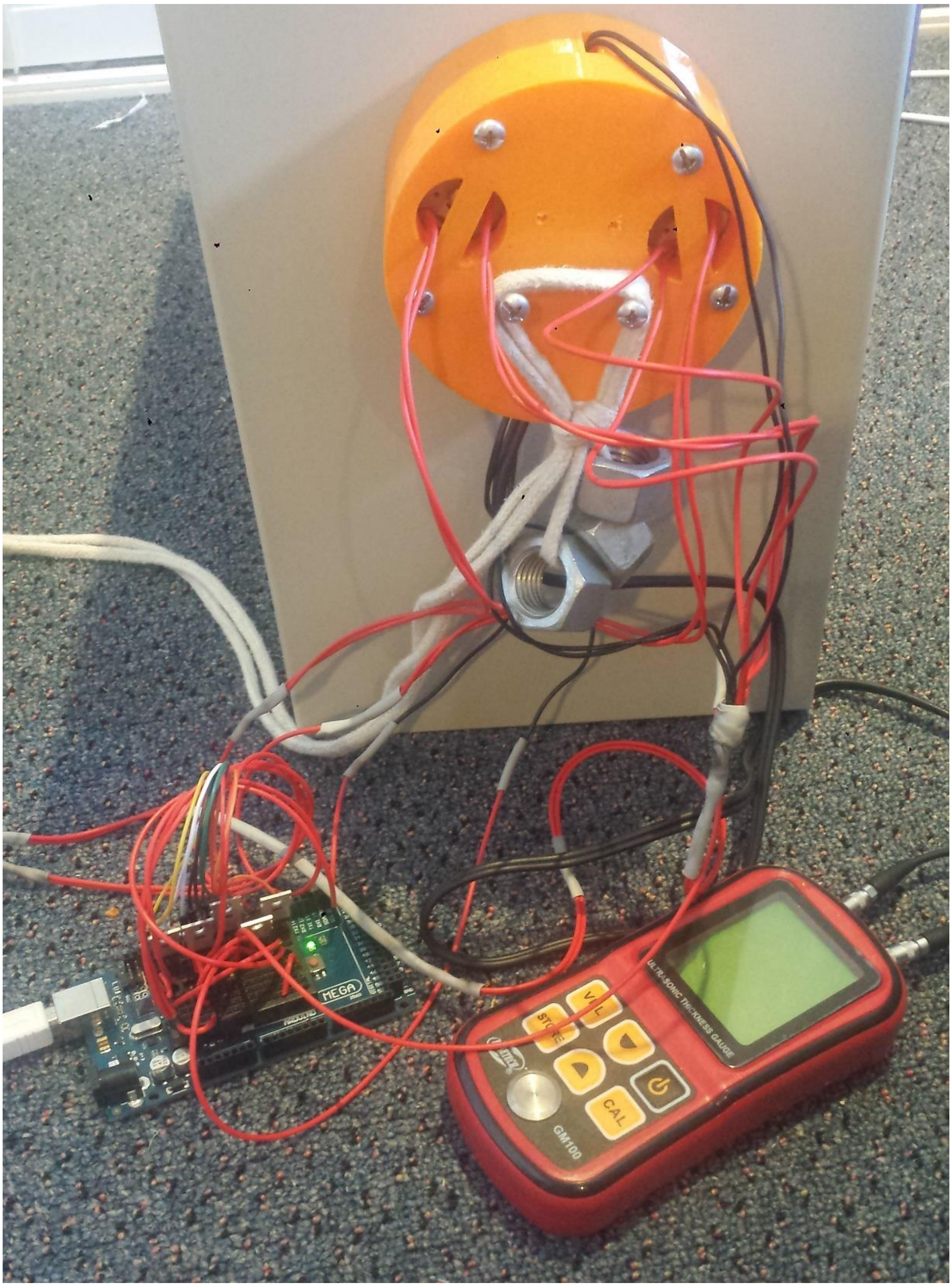

Figure 4.1.1b: Hardware Simulation Setup

4.1.2 Quadrotor Software Simulation

For the quadrotor side of the project, a software simulation was chosen due to budget (costs of and risks to UAV(s)/equipment). The intention of this part of the project was to gauge the effect of mounting the transducer assembly on the dynamics of a simple quadrotor.

This was done by simplifying the model of the attached assembly as a weight about its approximate centroid, in its expected position relative to the quadcopter. The hardware simulation module weighs approximately 320 grams with no vibration motors installed, so this region of weight was mass to be tested as a disturbance to an existing quadrotor model.

Using Quadrotor_Simulation_Complete, a complete SimMechanics model of the DJI F450 by Khanh Dang as a base, a 25mm sphere was placed via a rigid transform relative to the body, equidistant between two rotors, at the same radius as the rotors.

The added weight was incremented from 12.5 grams to 400 grams by factors of two. The addition of a counter-weighted pair was also added tested from 25 to 800 grams.

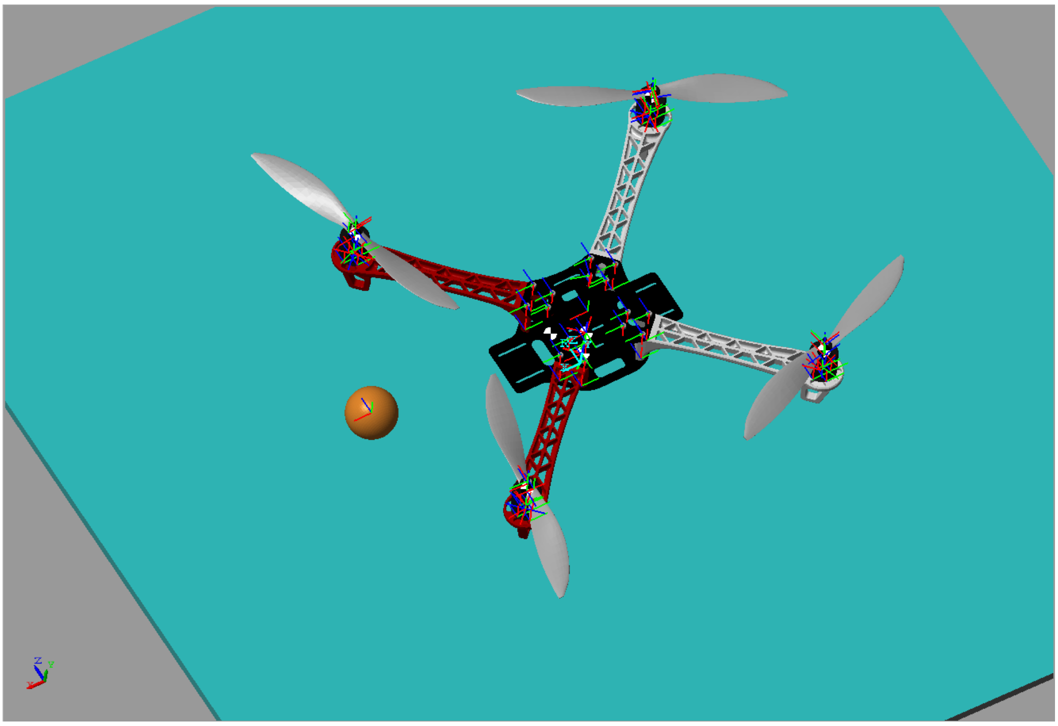

Figure 4.1.2a: SimMechanics rendering with sphere to simulate transducer

4.2 Design of Metrics and Regression Analysis

Using MATLAB's regression toolbox, a multivariable least squares linear regression was performed on the

a. success of adhesion of the assembly
b. success of phonetic coupling of the transducer, and

c. the error of thickness measurement,
   against the predictor values of

a. weight applied, and
b. vibration applied
c. material thickness

The SimMechanics software simulation model has many factors contributing to the outcome variables:

a. Propeller 1 angular velocity
b. Propeller 2 angular velocity
c. Propeller 3 angular velocity
d. Propeller 4 angular velocity
e. Altitude
f. Pitch
g. Roll
h. Yaw
i. X Position
j. Y Position

However, the complex interrelation of these factors means that performing a regression analysis on this data using the simulated transducer weight as a predictor variable is prone to produce a low-precision or misleading correlation. Instead a qualitative analysis was performed.

5. Results

5.1 Hardware simulation

	Duty Cycle(% of Combined Total)																				
Total Mass of Assembly(g)	0	5	10	15	20	25	30	35	40	45	50	55	60	65	70	75	80	85	90	95	100
390	1	1	1	1	1	1	1	0	0	0	0	0	0	0	0	0	0	0	0	0	0
448	1	1	1	1	1	0	0	0	0	0	0	0	0	0	0	0	0	0	0	0	0
506	1	1	1	1	0	0	0	0	0	0	0	0	0	0	0	0	0	0	0	0	0
564	0	0	0	0	0	0	0	0	0	0	0	0	0	0	0	0	0	0	0	0	0
622	0	0	0	0	0	0	0	0	0	0	0	0	0	0	0	0	0	0	0	0	0
680	0	0	0	0	0	0	0	0	0	0	0	0	0	0	0	0	0	0	0	0	0
738	0	0	0	0	0	0	0	0	0	0	0	0	0	0	0	0	0	0	0	0	0
796	0	0	0	0	0	0	0	0	0	0	0	0	0	0	0	0	0	0	0	0	0
854	0	0	0	0	0	0	0	0	0	0	0	0	0	0	0	0	0	0	0	0	0
912	0	0	0	0	0	0	0	0	0	0	0	0	0	0	0	0	0	0	0	0	0
970	0	0	0	0	0	0	0	0	0	0	0	0	0	0	0	0	0	0	0	0	0
1028	0	0	0	0	0	0	0	0	0	0	0	0	0	0	0	0	0	0	0	0	0
1086	0	0	0	0	0	0	0	0	0	0	0	0	0	0	0	0	0	0	0	0	0
1144	0	0	0	0	0	0	0	0	0	0	0	0	0	0	0	0	0	0	0	0	0
1202	0	0	0	0	0	0	0	0	0	0	0	0	0	0	0	0	0	0	0	0	0
1260	0	0	0	0	0	0	0	0	0	0	0	0	0	0	0	0	0	0	0	0	0
1318	0	0	0	0	0	0	0	0	0	0	0	0	0	0	0	0	0	0	0	0	0

Table 5.1a: Adhesion (1.5mm)

		Duty Cycle(% of Combined Total)																				
		0	5	10	15	20	25	30	35	40	45	50	55	60	65	70	75	80	85	90	95	##
Total Mass of Assembly(g)	390	1	1	1	1	1	1	1	1	1	1	1	1	1	1	1	1	1	1	1	1	1
	448	1	1	1	1	1	1	1	1	1	1	1	1	1	1	1	1	1	1	1	1	1
	506	1	1	1	1	1	1	1	1	1	1	1	1	1	1	1	1	1	1	1	1	1
	564	1	1	1	1	1	1	1	1	1	1	1	1	1	1	1	1	1	1	1	1	1
	622	1	1	1	1	1	1	1	1	1	1	1	1	1	1	1	1	1	1	1	1	1
	680	1	1	1	1	1	1	1	1	1	1	1	1	1	0	1	0	0	0	0	0	0
	738	1	1	1	1	1	1	1	1	1	1	1	0	0	0	0	0	0	0	0	0	0
	796	1	1	1	1	1	1	1	1	1	1	0	0	0	0	0	0	0	0	0	0	0
	854	1	1	1	1	1	1	0	0	0	0	0	0	0	0	0	0	0	0	0	0	0
	912	1	1	1	1	1	1	1	0	0	0	0	0	0	0	0	0	0	0	0	0	0
	970	1	1	1	1	1	1	1	0	0	0	0	0	0	0	0	0	0	0	0	0	0
	1028	1	1	1	1	1	1	1	0	0	0	0	0	0	0	0	0	0	0	0	0	0
	1086	1	1	1	1	1	0	0	0	0	0	0	0	0	0	0	0	0	0	0	0	0
	1144	1	1	1	1	1	0	0	0	0	0	0	0	0	0	0	0	0	0	0	0	0
	1202	1	1	1	1	1	0	0	0	0	0	0	0	0	0	0	0	0	0	0	0	0
	1260	1	1	1	1	1	0	0	0	0	0	0	0	0	0	0	0	0	0	0	0	0
	1318	0	0	0	0	0	0	0	0	0	0	0	0	0	0	0	0	0	0	0	0	0

Table 5.1b: Adhesion (15mm)

The Ultrasonic transducer failed to couple under all circumstances, so there is no coupling or thickness error data available.

5.2 Software Simulation

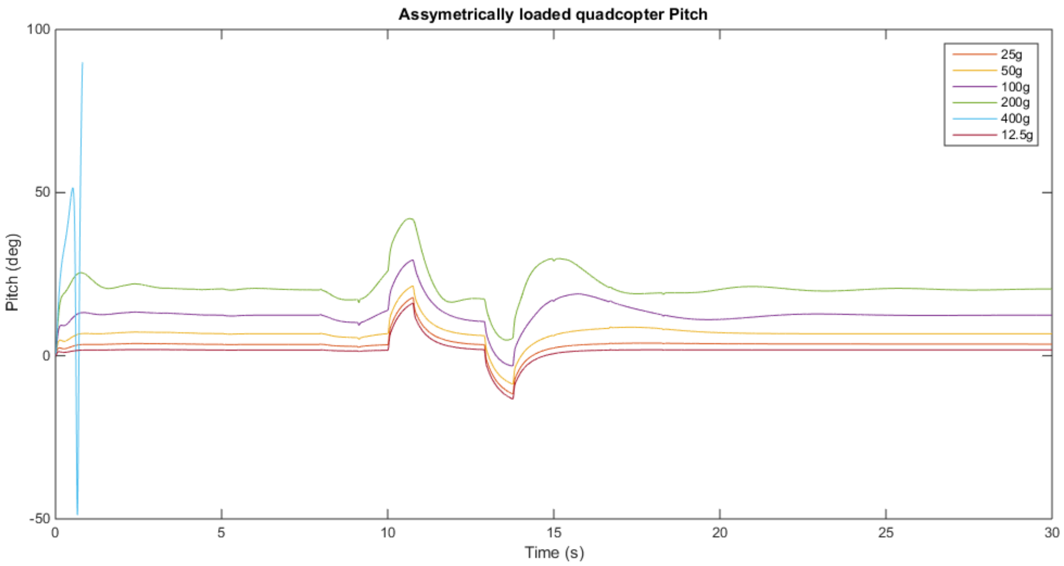

Figure 5.2a: Asymmetrically loaded quadcopter pitch

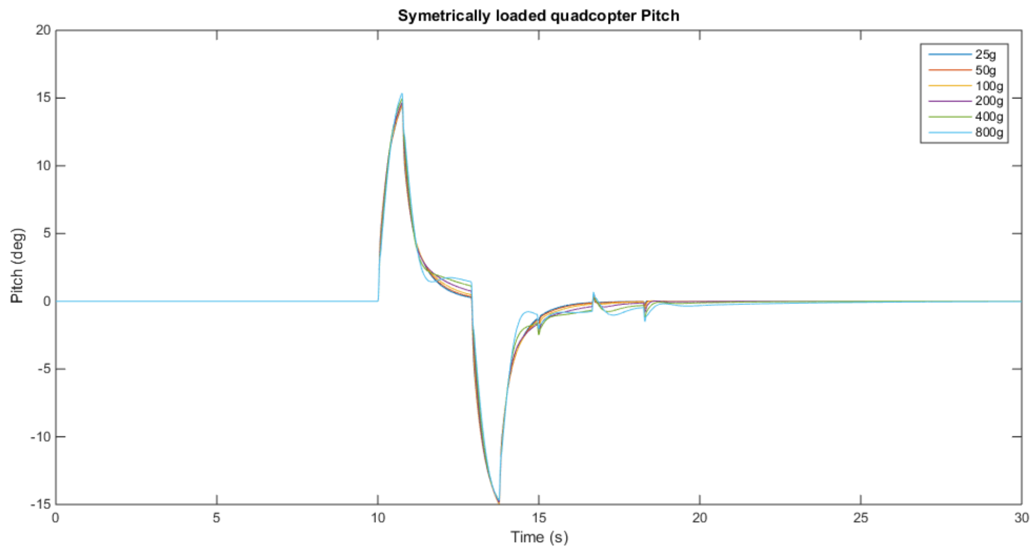

Figure 5.2b: Symmetrically loaded quadcopter pitch

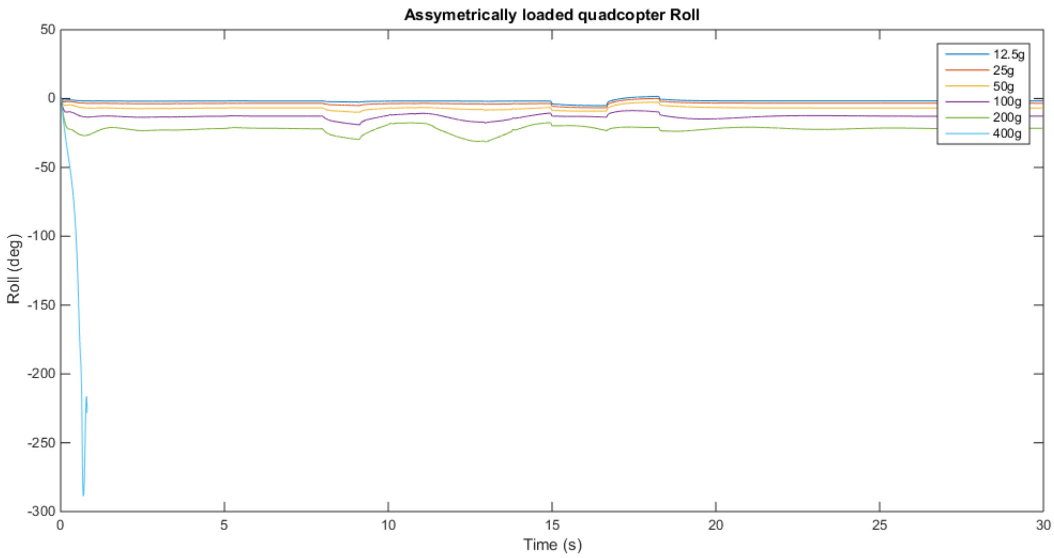

Figure 5.2c: Asymmetrically loaded quadcopter roll

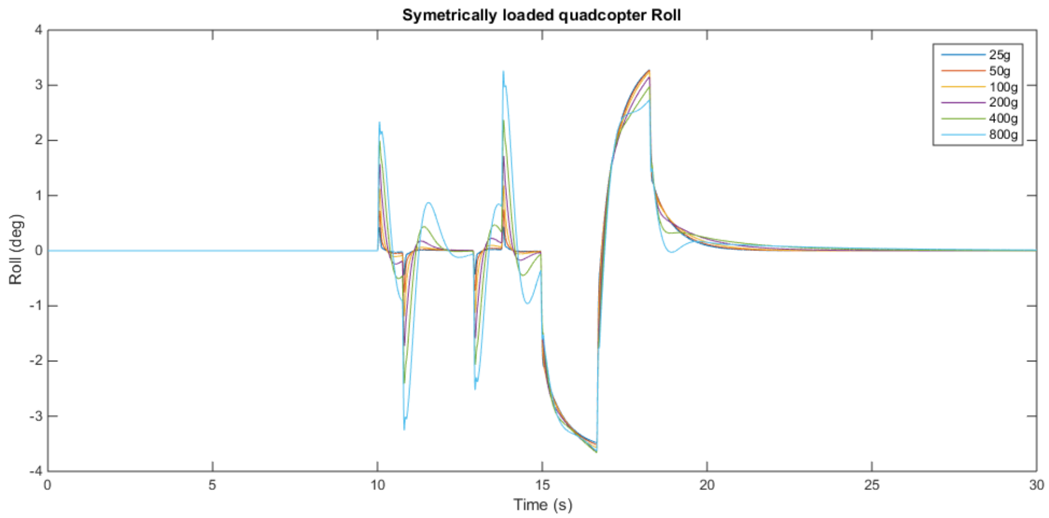

Figure 5.2d: Symmetrically loaded quadcopter roll

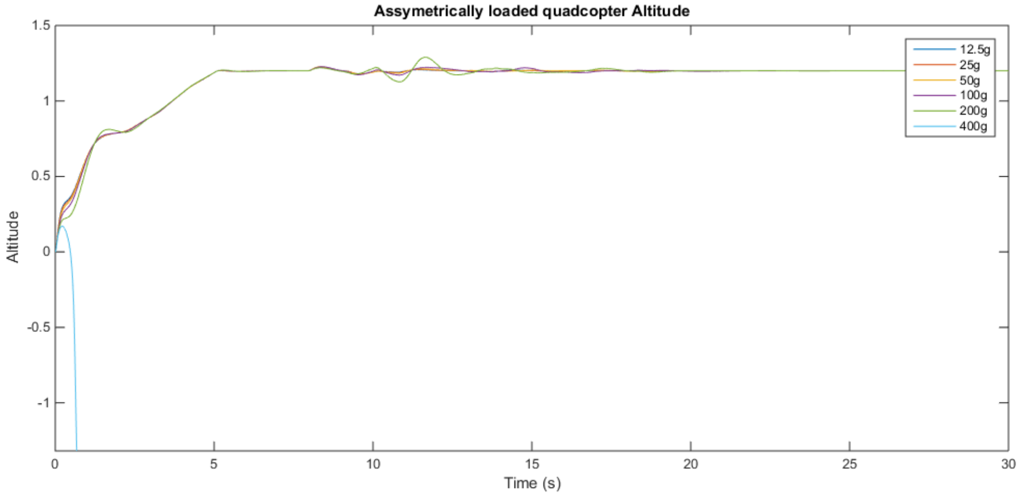

Figure 5.2e: Asymmetrically loaded quadcopter Altitude

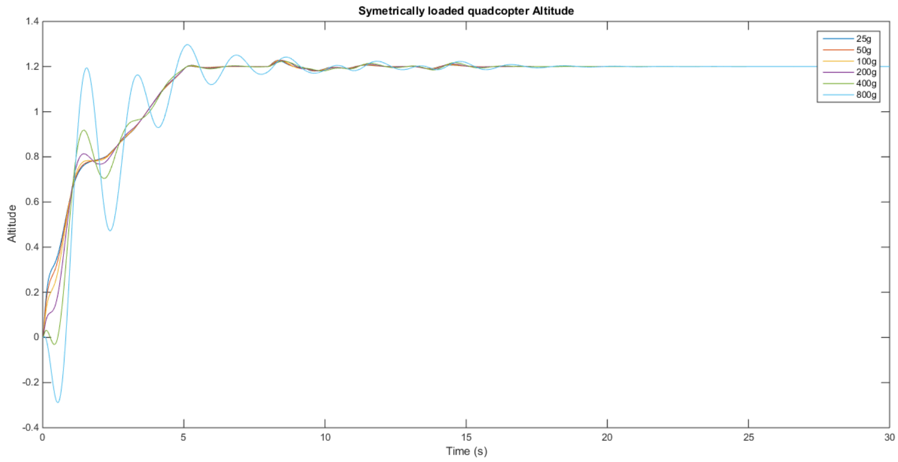

Figure 5.2f: Symmetrically loaded quadcopter altitude

5.3 Regression

$$Adhesion(binary, 1.5mm\ steel) = 0.33641 - 0.00023m - 0.00188v \qquad (5.3a)$$

$$Adhesion(binary, 15mm\ steel) = 1.8706 - 0.00113m - 0.00768v \qquad (5.3b)$$

$$Adhesion(binary) = 0.80376 - 0.00067m - 0.00482v + 0.03579p \qquad (5.3c)$$

$$m = transducer\ assembly\ mass\ (g)$$
$$v = vibration\ motor\ combined\ duty\ cycle(\%)$$
$$p = plate\ thickness(mm)$$

6. Discussion

6.1 Hardware Simulation

The hardware simulation exhibited a clear correlation between all of the contributing variables to the successful adhesion to the plate, shown in the regression models in section 5.3. It should be noted that almost all of the predictor variables for those linear regression models had t-values of greater than 10, and a confidence interval of greater than 99% as a result.

This test did come with the inherent obscurity of using vibration motors. As a vibration motor uses its angular velocity to make the vibration, the vibration motor will increase its amplitude and frequency at the same time, making the distinction of the individual effect of these variables and their effect on the outputs difficult. An example of this obscurity can be seen in table 5.1b, where the assembly, when loaded to 680 grams fails to adhere at 65% vibration, but successfully adheres at 70% vibration. Lower frequency differential harmonics were actually the cause of this, even though the table does not reflect this.

Although the outcome of the hardware simulation was recorded as a binary outcome, it was observed that in spite of a discrete failure to adhere to the vertical surface, some of the instances still provided varying levels of adherence, which in a field application may not be considered a functional failure, with the combined use of frictive material, and partial thrust from the rotors of a multi-copter.

It should be noted that the thickness testing module failed due to a variety of probably causes, including inadequate contact and/or impedance due to the assembly and transducer shape, low SNR due to low power and/or manufacturing quality, all which affect the overall feasibility of the appliance. Unfortunately, any other suitable thickness testing modules were far more expensive.

The quality of the electromagnets may have been detrimental to the hardware simulation as well, causing the assembly to be more sensitive to orientation than the design would have accounted for. However, this effect was not tested.

6.2 Software Simulation

The software simulation provided some useful information as to how an attached transducer assembly may affect the flight characteristics of a quadcopter UAV. The systems with larger attached mass increase the response time of the craft, as expected. Those with a counterweight opposite the transducer generally do this only, with no other effects, other than increases propeller speed.

Asymmetrically loaded crafts generally had this effect to a greater degree, as well as drifting towards the transducer assembly. On the pitch roll axes, there was more transient activity also. A comparison of the motor speeds also indicates that the asymmetrically loaded assembly requires a higher propeller speed if there are changes in the angular dimension(s) that the transducer creates a disturbance in. Depending on the application(in the case of a cylindrical vessel, it may be expected that only small changes in pitch and roll are made, whereas the yaw and attitude may vary quite a lot) it may be more suitable to use a single unbalanced or partially counter-weighted transducer assembly over a fully counter-weighted one.

The simulation ran into a singularity while processing an unbalanced transducer assembly weight of 400 grams. Using such a setup more successfully would have required redesigning the controller for the UAV, or at the very least tuning it to accommodate for the weight.

7. Conclusion

The thesis concluded that:

- The adhesion of a transducer assembly to a steel surface will depend on the surfaces thickness, any vibration, as well as the weight and moments present on the assembly due to the craft.
- Adhesion is feasible with small electromagnets.
- Using non-expensive components to discern the wall thickness in a field setup will prove highly sensitive to internal and external factors.
- It is likely that an ultrasonic thickness testing appliance on the UAV platform will require a custom flight controller.

8. Reference List

[1] T. Nelligan, "Ultrasonic NDT," *Quality,* vol. 30, p. 24, 1991.

[2] J. R. Davis, *Corrosion : Understanding the Basics*. Materials Park, OH, USA: A S M International, 2000.

[3] "Best Practice For The Procurement And Conduct Of Non-Destructive Testing," in *Manual Ultrasonic Inspection*, ed. United Kingdom: Health and Safety Executive - Gas And Process Safety Technology Division, 2000.

[4] J. Cullerne, "Ultrasonic Imaging," in *The Penguin dictionary of physics*, ed London, United Kingdom: Penguin, 2009.

[5] J. P. Woodcock and A. Hospital Physicists, *Ultrasonics* vol. 1. Bristol: Hilger [for] the Hospital Physicists' Association, 1979.

[6] T. Nelligan. (24/4/2015). *An Introduction to Ultrasonic Flaw Detection*. Available: http://www.olympus-ims.com/en/applications-and-solutions/introductory-ultrasonics/introduction-flaw-detection/

[7] (2015, 24/4/2015). *Combined Image Formats*. Available: http://www.olympus-ims.com/en/ndt-tutorials/instrumententation/combined/

[8] "Scorpion remote access tank shell inspection | Ultrasonic Crawler," ed. Online: Silverwing NDT, 2015.

[9] L. Hyon, P. Jaemann, L. Daewon, and H. J. Kim, "Build Your Own Quadrotor: Open-Source Projects on Unmanned Aerial Vehicles," *Robotics & Automation Magazine, IEEE,* vol. 19, pp. 33-45, 2012.

[10] T. Luukkonen, "Modelling and control of quadcopter," *Independent research project in applied mathematics, Espoo,* 2011.

[11] S. Tadakamadla and B. Oelmann, "Indoor local positioning system for ZigBee, based on RSSI," 2006.

[12] N. B. Priyantha, "The cricket indoor location system," Massachusetts Institute of Technology, 2005.

[13] S. Weiss, D. Scaramuzza, and R. Siegwart, "Monocular-SLAM–based navigation for autonomous micro helicopters in GPS-denied environments," *Journal of Field Robotics,* vol. 28, pp. 854-874, 2011.

[14] M. Achtelik, A. Bachrach, R. He, S. Prentice, and N. Roy, "Stereo vision and laser odometry for autonomous helicopters in GPS-denied indoor environments," in *SPIE Defense, Security, and Sensing*, 2009, pp. 733219-733219-10.

[15] L. Ojeda and J. Borenstein, "Personal dead-reckoning system for GPS-denied environments," in *Safety, Security and Rescue Robotics, 2007. SSRR 2007. IEEE International Workshop on*, 2007, pp. 1-6.

[16] *Model aircraft and RPA,* C. A. S. Authority, 2014.

[17] J. S. Cavote, "Drones Promise Faster, Easier Inspection of Boilers, Stacks, Towers, and More - POWER Magazine," in *PowerMag*, ed. Online: PowerMag, 2014.

[18] E. W. Hawkes, D. L. Christensen, E. V. Eason, M. A. Estrada, M. Heverly, E. Hilgemann*, et al.*, "Dynamic surface grasping with directional adhesion," in *Intelligent Robots and Systems (IROS), 2013 IEEE/RSJ International Conference on*, 2013, pp. 5487-5493.

[19] J. Craighead, R. Murphy, J. Burke, and B. Goldiez, "A survey of commercial & open source unmanned vehicle simulators," in *Robotics and Automation, 2007 IEEE International Conference on*, 2007, pp. 852-857.

[20] S. R. B. dos Santos, S. N. G. Junior, C. L. N. Júnior, A. Bittar, and N. M. F. de Oliveira, "Modeling of a hardware-in-the-loop simulator for Uav autopilot controllers," in *Proceedings of the 21st Brazilian Congress of Mechanical Engineering*, 2011.

[21] A. Gibiansky, "Title," unpublished|.

[22] K. Dang. (2014). *Simulate Quadrotor in Simulink with SimMechanics*. Available: http://au.mathworks.com/matlabcentral/fileexchange/48052-simulate-quadrotor-in-simulink-with-simmechanics

[23] R. A. Serway, *Physics for Scientists and Engineers*, 2nd ed.: Saunders College Publishing, 1986.
[24] J. H. Aldrich and F. D. Nelson, *Linear probability, logit, and probit models* vol. 45: Sage, 1984.
[25] S. H. Brown, "Multiple linear regression analysis: a matrix approach with matlab," *Alabama Journal of Mathematics,* vol. 34, pp. 1-3, 2009.

9. Appendices

9.1 Risk Assessment

Name of Test: Procuring and Testing design assembly on quadcopter drone

Purpose: Thesis design testing			
Operator:		**Duration:** 2 hours	
SDS Attached:	No	No **x**	N/A
Major Hazard Types: (Tick at least one)			
Chemical		Mechanical **x**	
Electrical		Thermal **x**	
Environmental		Other:	

SUMMARY OF RISKS

Specific Task/Activity	Potential Hazards/Consequences	Assessed Risk	Risk Control Measures	Reassessed Risk
Flying Copter drone	Collision of large, expensive drone with human or environment	High	Only CASA registered pilots may fly the expensive drones. Safety glasses are to be worn when in close proximity	Medium
Operating or servicing Copter drone	Fire as a result of Copter battery failure	Medium	Disconnect batteries where necessary	Low
Soldering or 3D printing	Burns	Medium	Safety glasses, General caution when handling hot solder or plastic	Medium-Low

		Consequence →				
		Near hit, no injury. No $ lost or damage	First Aid treatment required for a minor injury Property damaged but can still operate	Medical treatment OR lost time injury. Property damaged but can be fixed immediately	Serious injury requiring admission to hospital OR permanent disabling injury. Notifiable to regulatory Authority. Equipment damaged	Fatality, maximum high level headline exposure and loss of credibility. Equipment damaged/destroyed
Likelihood		Insignificant	Minor	Moderate	Major	Severe

It is expected to occur in most circumstances e.g. Daily	Almost certain	Medium	High	Extreme	Extreme	Extreme
Will probably occur in most circumstances. e.g. weekly	Likely	Medium	Medium	High	Extreme	Extreme
Might occur at some time e.g. Annually	Possible	Low	Medium	Medium	High	Extreme
Probably won't, but could occur at some time. e.g. once every 5 years	Unlikely	Low	Medium	Medium	Medium	High
May occur in exceptional circumstances.	Rare	Low	Low	Low	Medium	Medium

9.2 Gantt Chart

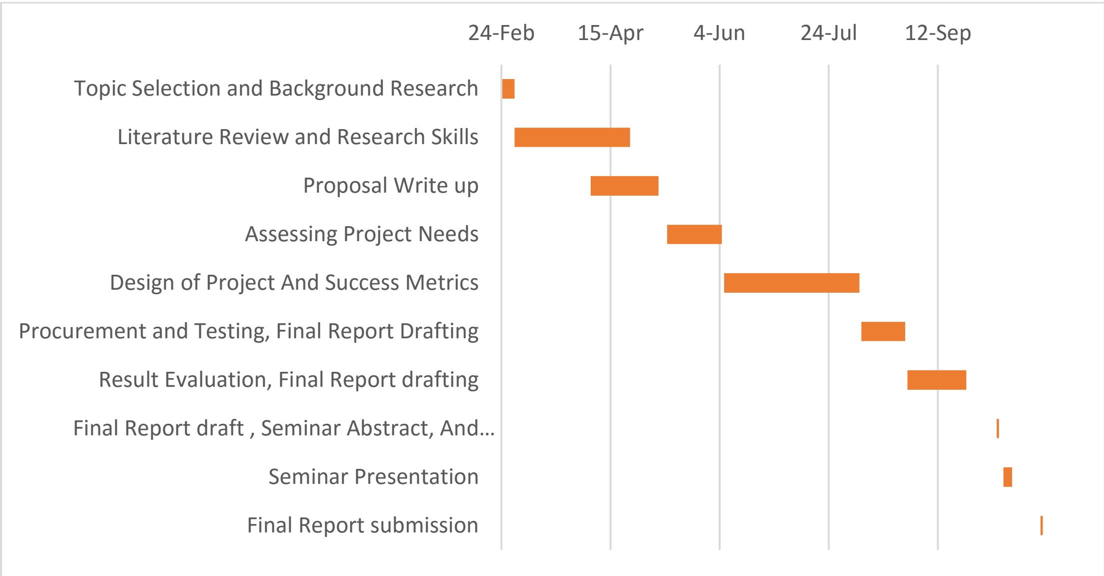

9.3 SimMechanics simulation inputs

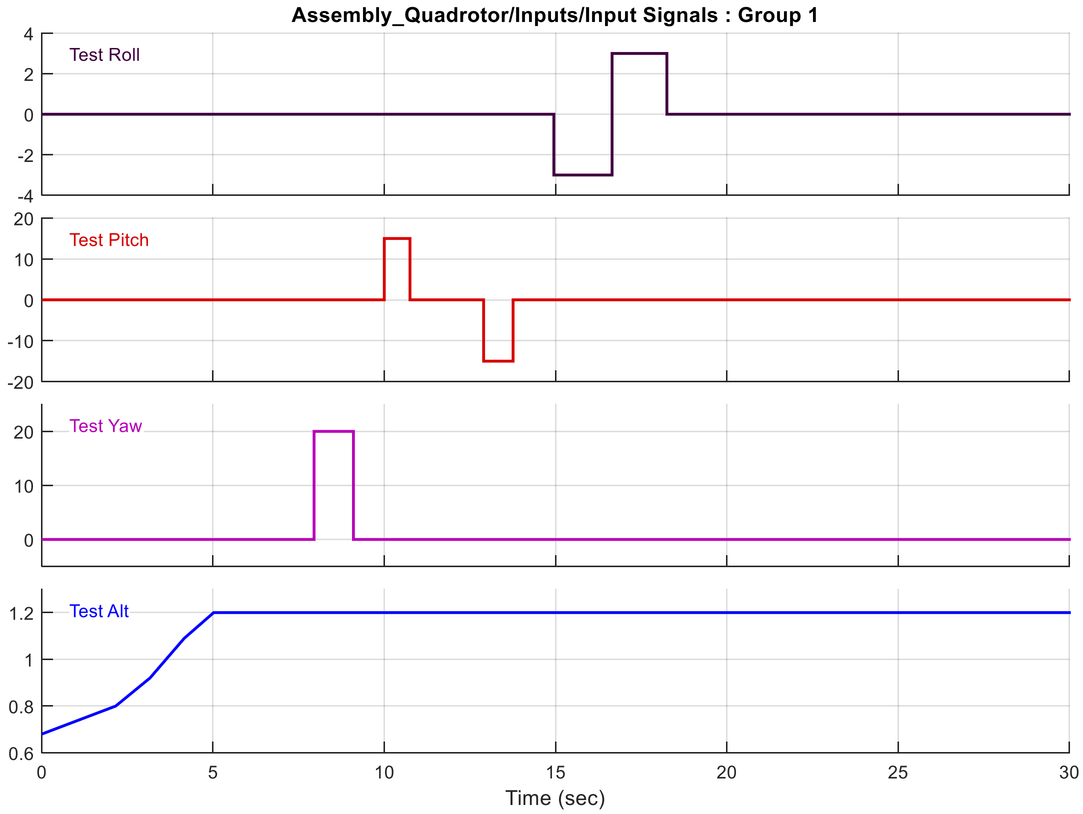

Figure 9.3a: SimMechanics simulation inputs

9.4 Motor 1 Speed (Combined Symmetrical and Asymmetrical)

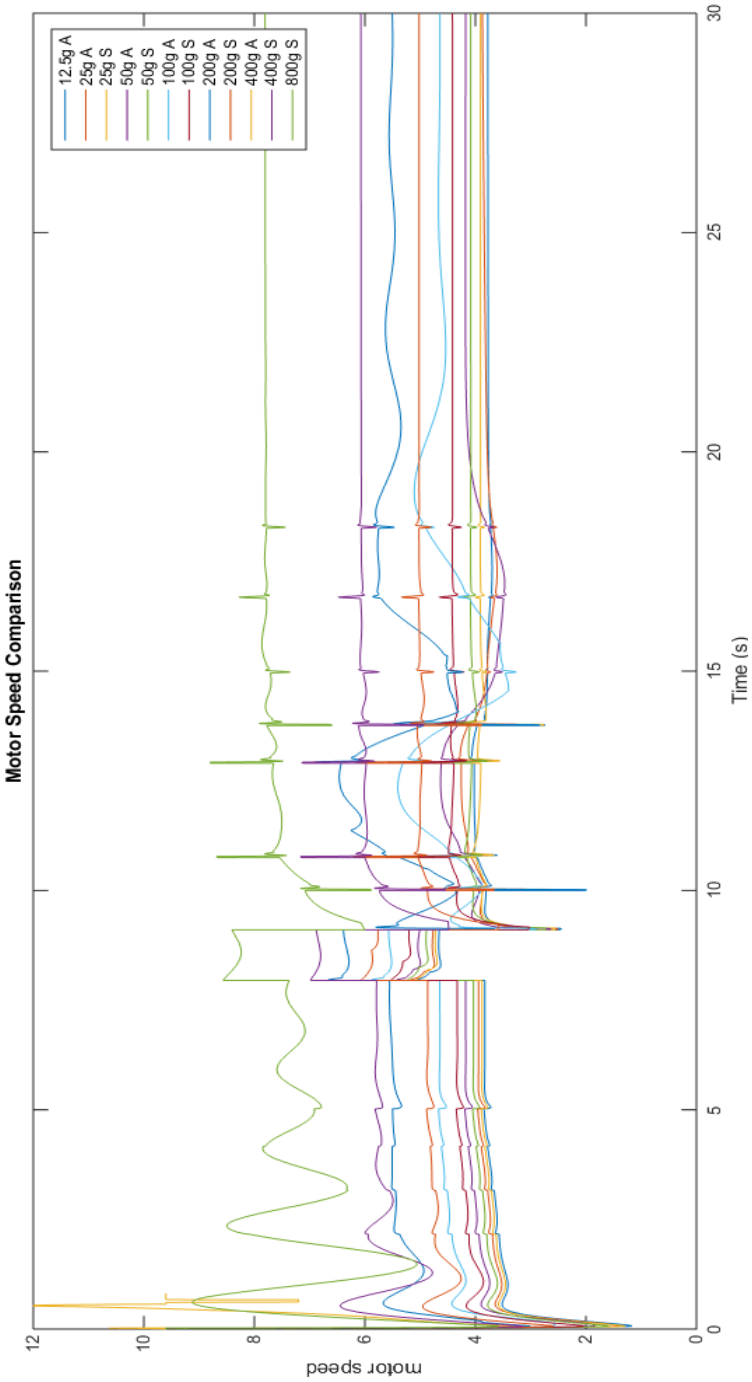

Figure 9.4a: Motor 1 Speed (Combined Symmetrical and Asymmetrical)